Reprint Series
26 February 1993, Volume 259, pp. 1277–1282

SCIENCE

Mediterranean Outflow Mixing Dynamics

James F. Price,* Molly O'Neil Baringer, Rolf G. Lueck, Gregory C. Johnson, Isabel Ambar, Gregorio Parrilla, Alian Cantos, Maureen A. Kennelly, and Thomas B. Sanford

Mediterranean Outflow Mixing and Dynamics

James F. Price,* Molly O'Neil Baringer, Rolf G. Lueck, Gregory C. Johnson, Isabel Ambar, Gregorio Parrilla, Alain Cantos, Maureen A. Kennelly, Thomas B. Sanford

The Mediterranean Sea produces a salty, dense outflow that is strongly modified by entrainment as it first begins to descend the continental slope in the eastern Gulf of Cadiz. The current accelerates to 1.3 meters per second, which raises the internal Froude number above 1, and is intensely turbulent through its full thickness. The outflow loses about half of its density anomaly and roughly doubles its volume transport as it entrains less saline North Atlantic Central water. Within 100 kilometers downstream, the current is turned by the Coriolis force until it flows nearly parallel to topography in a damped geostrophic balance. The mixed Mediterranean outflow continues westward, slowly descending the continental slope until it becomes neutrally buoyant in the thermocline where it becomes an important water mass.

The deep ocean is filled with water masses that originate in marginal seas where a cold or dry continental climate can produce dense water by intense and sustained air-sea interaction (*1*). This dense water forms bottom currents that flow out from the marginal seas and settle in the open ocean at levels that are determined by their relative densities (*2*, *3*). The temperature, salinity, and other chemical properties of these outflows set the climate of the deep sea, which is known to have been significantly different in other epochs (*4*) from what it is today. One step toward better interpretation of the record of past deep-sea climate change or toward prediction of future climate change is to understand what processes set the properties of these marginal sea outflows.

We examined the outflow that begins in the Mediterranean basin where the loss of freshwater by evaporation causes Mediterranean seawater to have a high salinity, S = 38.4 psu (practical salinity units, nearly equal to parts per thousand), and consequently a high density, σ_θ = 28.95 kg m^{-3} (*5*). This density exceeds that of North Atlantic bottom water, $\sigma_\theta \simeq 27.95$ kg m^{-3}, and is much greater than the density of North Atlantic surface water found just outside the Mediterranean. The resulting horizontal contrast in density drives an inverse estuarine circulation through the shallow and narrow Strait of Gibraltar (Fig. 1). Fresher and lighter Atlantic surface water forms the inflowing upper layer that is transformed by freshwater loss into saline, dense Mediterranean water that forms the outflowing lower layer (*6*). The Mediterranean outflow spills over the shallow sills in the Strait of Gibraltar and cascades down the continental shelf and slope into the Gulf of Cadiz and the open North Atlantic (Fig. 2).

Despite its initially very high density, the Mediterranean outflow water does not reach the bottom of the North Atlantic because it entrains (*7*) a substantial volume of the overlying North Atlantic Central water while still in the Gulf of Cadiz. Entrainment reduces the high salinity and density of the outflow, and the resultant mixed Mediterranean water that finally reaches the open North Atlantic has a density $\sigma_\theta = 27.6 \pm 0.1$ kg m^{-3} that makes it neutrally buoyant at depths of about 800 to 1300 m in the main thermocline (*8*–*13*). Mixed Mediterranean water is considerably

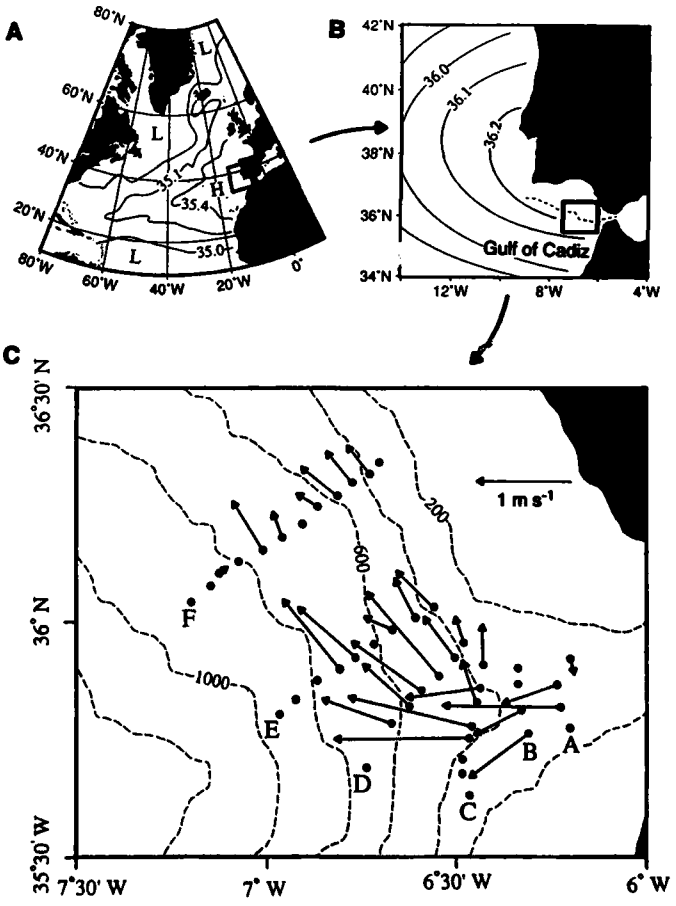

Fig. 1. (**A**) North Atlantic salinity distribution (in practical salinity units, H and L mark highs and lows) on a density surface that is near the salinity maximum of the Mediterranean outflow (its depth is 1200 m in the tropical and subtropical North Atlantic, and it reaches the sea surface in the Norwegian Sea and in shelf waters northwest of the Gulf Stream). A high-salinity tongue of mixed Mediterranean water originates from the northern Gulf of Cadiz and extends west across the North Atlantic basin and north toward the Norwegian Sea. The other water masses at this density level all have lower salinity (Labrador Sea water in the northwest, surface water of Arctic origin in the northwestern Norwegian Sea, and Antarctic Intermediate water to the south). [Adapted from figure 2 of (*14*)] (**B**) Salinity in the eastern North Atlantic and Gulf of Cadiz at a depth of 1200 m. The dashed line running through the Strait of Gibraltar denotes the axis of the outflow that is shown in vertical section in Fig. 2A. [Adapted from (*36*)] (**C**) The maximum observed velocity of outflow currents in the eastern Gulf of Cadiz as measured by expendable current profilers (XCPs). The lines of stations that make up sections are labeled A through F in order of increasing distance away from the Strait of Gibraltar. Note that the outflow current crossed isobaths (dashed lines, depth in meters) toward deeper water in the vicinity of section C and was more or less parallel to the local isobaths near sections E and F.

J. F. Price and M. O'Neil Baringer are at the Woods Hole Oceanographic Institution, Woods Hole, MA 02543. R. G. Lueck is at the School of Earth and Ocean Sciences, University of Victoria, Victoria, British Columbia, V8W 3P6, Canada. G. C. Johnson and T. B. Sanford are at the Applied Physics Laboratory and School of Oceanography, University of Washington, Seattle, WA 98105. I. Ambar is at the Grupo de Oceanografia, University of Lisbon, 1200 Lisbon, Portugal. G. Parrilla is at Instituto Español Oceanografia, 28002 Madrid, Spain. A. Cantos is at AINCO-Interocean, 28016 Madrid, Spain. M. A. Kennelly is at Planning Systems Inc., McLean, VA 22102.

*To whom correspondence should be addressed.

saltier and warmer than thermocline water masses that have subpolar origins and makes a conspicuous anomaly that extends southwest across the subtropical North Atlantic and north along the eastern boundary of the northern North Atlantic (Fig. 1A) (*14*).

A Field Survey of the Mediterranean Outflow

We conducted an intensive field survey of the northern Gulf of Cadiz in the fall of 1988 to characterize the physical dynamics of the Mediterranean outflow and, more specifically, to learn where and how the outflow is modified by mixing. The field data include 99 full-depth profiles of temperature and salinity, $T(z)$ and $S(z)$, that were made with a conductivity, temperature, and depth instrument (CTD) (*15*). At 56 of the CTD stations, we obtained a profile of the horizontal current, $U(z)$, with an expendable current profiler (XCP) (*16*) (Fig. 3) and, at 29 of those stations, a profile of turbulence intensity with an expendable dissipation profiler (XDP) (*17*) (Fig. 4).

About two thirds of the CTD stations were laid out in the Gulf of Cadiz in eight sections that were oriented across the path of the outflow (labeled A through H in Figs. 1C and 2A). We found these data to be similar to hydrographic data acquired in similar surveys that have been conducted since the 1960s (*18*).

We estimated the transport of volume, salinity, and density through each of the sections (Fig. 5) by combining the CTD and XCP current data. By analyzing the transport data, we calculated a transport-weighted average salinity for each section, S_{Twtd}, defined as the salinity transport in the outflow divided by the volume transport, which should give a clear and representative measure of salinity variation along the outflow path (Fig. 2B). As expected, S_{Twtd} has an initial value of 38.4 psu in the Mediterranean Sea and decreases gradually as the outflow crosses the main sill at Camarinal (5°46'W). A corresponding gradual change is evident in the transport profiles (Fig. 5) at sections A and B, which are near the Strait of Gibraltar, and show that the upper portion of the outflow water begins to mix with the overlying North Atlantic water while still in the strait (*19*).

The value of S_{Twtd} then decreases rapidly to about 36.6 psu at section D, which is accompanied by a significant change in the transport profiles: from sections B to E, there is an increase of about 0.6×10^6 m^3 s^{-1} in the westward volume transport (outflow) of water in the density range σ_θ = 27.3 to 27.9 kg m^{-3}; from sections E to B, there is a complementary decrease in the eastward volume transport of North Atlantic water in the density range σ_θ = 27.0 to 27.2 kg m^{-3}. This is a result of the entrainment of North Atlantic Central water, which causes the volume transport of the outflow to roughly double and the value of S_{Twtd} to decrease rapidly in the region around sections C and D. Westward of section E, the continued change in S_{Twtd} and the transport profiles is fairly gradual, with S_{Twtd} decreasing to about 36.3 psu at section H in the extreme western Gulf of Cadiz.

The rate of change of salinity and density along the path of the outflow is strongly inhomogeneous. Roughly 50% of the net decrease in salinity and density occurs between sections B and E, which is only about 15% of the total path length in the Gulf of Cadiz. This is also the region where the outflow begins to descend the continental slope (Fig. 5A), which suggests that the mixing depends on bottom topography and, by inference, the dynamics of the current itself.

Elements of Outflow Dynamics

Laboratory studies provide considerable insight into the dynamics of density-driven currents (*20*, *21*). Even though no single laboratory experiment includes all of the

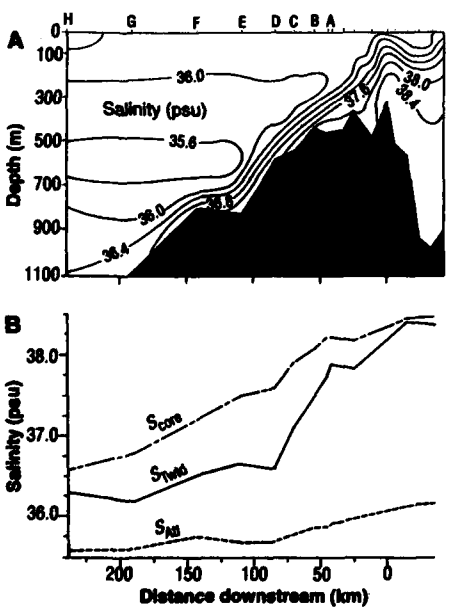

Fig. 2. (**A**) A salinity section along the axis of the outflow made with data from conductivity, temperature, and depth instruments (CTDs) (location of this section is shown as the dashed line in Fig. 1B). The origin (0 km downstream) is the main sill at Camarinal (5°46'W). This section is very similar to that produced by Heezen and Johnson (*8*) with data taken until about 1965. (**B**) Traditional core value, S_{core}, the maximum salinity within a section; the transport-weighted salinity within the outflow, S_{Twtd}, which we believe is a better measure of the average salinity of the outflow; and S_{All}, the salinity of the North Atlantic water just above the outflow. The values of S_{core} and S_{All} are nearly identical to those shown in figure 12 of (*8*).

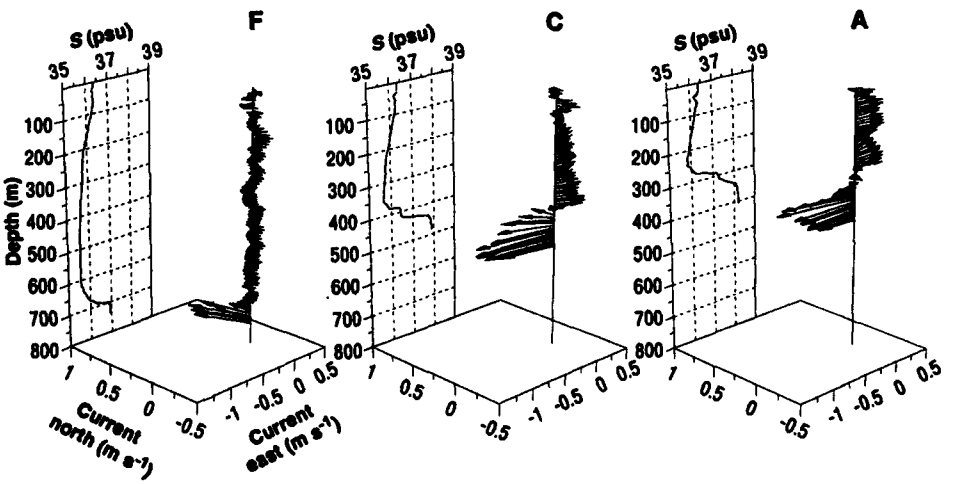

Fig. 3. Profiles of CTD-measured salinity and XCP-measured currents along the outflow axis at sections (from right to left) A, C, and F. The current profiles are viewed as if looking toward the northeast from a vantage point above the Gulf of Cadiz. The XCP profiles show a jetlike current of Mediterranean outflow water with a typical thickness of 100 m and a maximum speed from sections A to D of ~1 m s^{-1}. In most profiles, the current maximum was near the middle of the outflow layer, and there were generally thick shear layers in the interfacial boundary layer between the Mediterranean water and the inflowing North Atlantic water, and in the bottom boundary layer. The depth of the outflow increased from east to west as it descended the continental shelf and slope. The outflow current changed direction by about 90° and slowed considerably from sections C to F. The width of the outflow layer increased from about 10 km at section A to about 45 km at section F, so that the volume transport within the outflow layer increased by about a factor of 2 from sections A to F. The salinity profiles show a substantial decrease in the outflow salinity going from sections A to F. Within the outflow layer, the salinity (and density) profiles typically show a quasi-mixed layer near the bottom that is about half the total thickness of the outflow layer and a highly stratified interface layer of comparable thickness.

complexity of an oceanic outflow, we can nevertheless deduce some of the important elements of outflow dynamics from idealized examples. A simple but still relevant case is that of a source of constant buoyancy that feeds a density current that is descending a straight (nonrotating), inclined channel. The current accelerates down the slope until it reaches a quasi-steady state in which the pressure gradient along the stream is balanced by the retarding effect of bottom stress and entrainment stress.

The importance of the entrainment stress depends on the internal Froude number, $F = U/\sqrt{g'h}$ (*21*, *22*), where U is the current speed, $g' = g\Delta\rho/\rho_0$ is the reduced gravity, g is the acceleration of gravity, $\Delta\rho$ is the density difference between the density current and the ambient water (the density anomaly), ρ_0 is a reference density, and h is the thickness of the density current. The Froude number appears in many hydraulics problems and has several interpretations, including that it is the ratio of the current speed to the phase speed of long internal waves. If $F < 1$, the density current will not mix significantly with the overlying water. In that case, the retarding stress that balances the pressure gradient is mainly bottom stress. If $F > 1$, the entrainment stress may provide a significant part of the total stress. In that case, the density current will entrain the overlying water and consequently lose some of its density anomaly. This suggests that F is a crucial internal flow parameter of an outflow. Estimating F in a straightforward way from the CTD and XCP data, we found that $F \approx 1$ in the first 50 to 100 km of the outflow path and is significantly less over the next 100 km.

To understand why the Froude number of the outflow might exceed 1, we examined how the momentum balance changes along the path in response to variation of external parameters. The bottom stress on a turbulent current is often approximated by a quadratic drag law $\tau_b = \rho_0 C_D U^2$, where, for ocean bottoms, $C_D \approx (1.5 \text{ to } 3) \times 10^{-3}$, depending on the roughness of the terrain and the height at which U is observed. Under this approximation, it is easy to show that the Froude number of a quasi-steady density current will exceed 1 if $d_x + h_x \geq C_D$, where d_x and h_x are the along-stream slopes of the bottom depth and the layer thickness (*23*). This suggests that the bottom slope and the drag coefficient are important external parameters of a density current.

The terms in the momentum balance can also be estimated by an analysis of the data. The bottom and entrainment stresses can be inferred from models of boundary layer flow. We used the XCP measurements of the current in the lowest 5 to 10 m of the bottom boundary layer to estimate the bottom stress, τ_b, by fitting $U(z)$ to the logarithmic form $(U_*/k)\log(z/z_0)$, where $U_* = (\tau_b/\rho_0)^{1/2}$ is the friction velocity, which is to be determined, $k = 0.4$ is von Karman's constant, and z_0 is the roughness length (*24*). The estimated bottom stress is quite large and shows a systematic variation along the path that is roughly proportional to the variation of U^2: $\tau_b \approx 1.5$ Pa at sections A and B, has a maximum of about 2.5 Pa at section C, and is much less, about 0.3 Pa, at section F.

The XDP measurements of the turbulence intensity were used to estimate the profile of turbulent kinetic energy dissipation, $\epsilon(z)$. This too can be used to infer stress, with the assumption of a simplified energy budget, $\epsilon(z) \approx \tau(z)\, U_z$, where $\tau(z)$ is the turbulent stress and U_z is the vertical shear of the horizontal current, which can be readily estimated from XCP data (*25*). We used this method to estimate the ratio of the turbulent stress in the interfacial layer, τ_e, to the bottom boundary layer stress, $\Gamma = \tau_e/\tau_b$, and found that the mean value over 29 samples, distributed mainly between sections A and D, is $\Gamma = 0.4 \pm 0.2$, where the uncertainty is twice the standard error. Thus the bottom stress appears to exceed the entrainment stress by about a factor of 2 over that portion of the outflow path. There appears to be a spatial variation of Γ within this region, although the small number of samples together with the large variance of Γ render this somewhat tenuous. The mean (and median) at sections A and B is $\Gamma = 0.3 \pm 0.1$ (0.2) ($n = 9$); there appears to be a maximum at section C, where $\Gamma = 0.9 \pm 0.5$ (0.6) ($n = 11$), and a small decrease at section D, where $\Gamma = 0.6 \pm 0.6$ (0.4) ($n = 6$). The number of XDP samples from sections E and F is inadequate to yield a stable mean of Γ, but inspection of the dissipation profiles suggests that Γ may decrease further to the west.

The pressure gradient averaged over the outflow layer can be written as $P_x = g[(\Delta\rho h)_x + \Delta\rho d_x]$, where d is the bottom depth and the derivative, indicated by the subscript x, is taken along the direction of the outflow. The first term represents the internal (baroclinic) pressure gradient, which arises from variations in density or layer thickness along the outflow path. This term is dominant within the Strait of Gibraltar proper and drives the two-layer

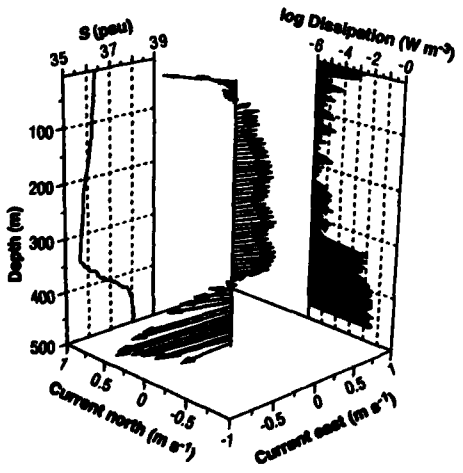

Fig. 4. A profile of current and salinity as in Fig. 3 and a profile of dissipation from an expendable dissipation profiler (XDP) (right panel). These data are from a typical station along the outflow axis at section C. Dissipation was extremely high in the saline outflow layer, of order 10^{-2} W m^{-3}, and was about a factor of 10^4 less in the inflowing Atlantic water above.

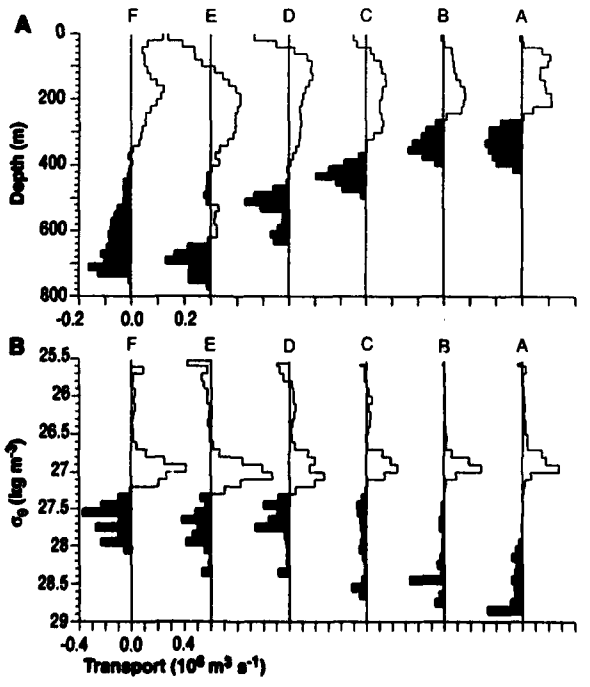

Fig. 5. (**A**) Volume transport across each of the sections shown as a function of depth. The outflow water is blackened. (**B**) Volume transport shown as a function of density (we use density rather than salinity because density is monotonically increasing with depth, while salinity has a local minimum in the Atlantic water just above the outflow layer). Note the large change in the transport profile as a function of density between sections B and E. This is evidence of entrainment by the outflow of North Atlantic Central water from the density range σ_θ = 27.0 to 27.2 kg m^{-3}.

exchange flow. Mediterranean water is forced westward through the strait at a speed of about 1 m s^{-1} [although the speed is highly dependent on the tidal phase within the strait; see (*19*) for a detailed discussion of the complex time-dependent hydraulic control phenomenon within the strait]. After the main sill at Camarinal, the Mediterranean water overflows another minor sill at 6°10'W, which is very close to our section A, and begins a monotonic descent into the Gulf of Cadiz.

Mediterranean Outflow Dynamics

Once the outflow enters the Gulf of Cadiz, the pressure gradient is increasingly dominated by the second term, the topographic term, and the outflow is very strongly affected by bottom topography, as earlier investigators have emphasized in different ways (*8*, *10*–*13*). Our description of the outflow dynamics is divided into three segments that are defined by the relation of the outflow current to the bottom topography.

Channel flow. At sections A and B, the Mediterranean outflow is constrained within a narrow channel ~10 km wide that runs west-southwest. This channel appears to be an extension of the Strait of Gibraltar that has been cut out of the continental shelf by the outflow current. The along-stream slope of the channel bottom is typical of a continental shelf, $d_x \approx (1 \pm 0.5) \times 10^{-3}$, where the large uncertainty indicates the variation on the scale of the outflow width. The rate of change of the layer thickness is similar; thus, $d_x + h_x \lesssim C_D$. The observed Froude number is also $\lesssim 1$, and, as we have seen, there is some mixing in this region, although it is not particularly strong.

The pressure force per unit area along the direction of the outflow is estimated to be $hP_x = hg\Delta\rho(d_x + h_x) \approx 3 \pm 1.5$ Pa, where $\Delta\rho \approx 1.5$ kg m^{-3}. This is a large force that would, if unbalanced by a stress, cause the outflow current to accelerate from about 1 m s^{-1} at section A to about 1.4 m s^{-1} by section B. No such acceleration is observed, evidently because this pressure force is largely balanced by the sum of the bottom stress, which is $\tau_b \approx 1.5$ Pa in this region, estimated from the fit to XCP data, and the entrainment stress, which is $\tau_e \approx 0.5$ Pa, estimated from the ratio τ_e/τ_b that was inferred from XDP and XCP data. The combined bottom and entrainment stress gives a retarding stress of $\tau \approx 2$ Pa, which appears sufficient to roughly balance the pressure force.

This first region of the outflow can thus be characterized as a more or less steady channel flow that has a Froude number of ~1. The bottom stress provides most of the retarding stress, evidently because the observed slopes do not exceed the drag coefficient.

Initial descent of the continental slope. The outflow reaches the edge of the continental shelf just west of section B. It flows directly across the much steeper continental slope near section C where $d_x \approx (11 \pm 2) \times 10^{-3}$, which is considerably larger than the drag coefficient. The observed internal Froude number reaches a maximum of about 1.3, and entrainment is much stronger here than just upstream.

The momentum balance is also quite different. The steep bottom slope causes a very large pressure force where the outflow first crosses onto the continental slope: $hg\Delta\rho d_x \approx 13$ Pa, where $\Delta\rho \approx 1.4$ kg m^{-3} is the initial value of the density anomaly. The current accelerates to a maximum speed of about 1.3 m s^{-1} at section C, which is, again, very much less than what would be expected from this pressure force. There appear to be three processes that limit the downhill acceleration of the current in this crucial region.

1) Turbulent stresses that arise from entrainment and bottom friction are very large and produce intense dissipation throughout the entire thickness of the outflow (Fig. 4). Many individual XDP profiles show two distinct dissipation maxima: an upper maximum in the interfacial boundary layer between the outflow and the overlying Atlantic water and a lower maximum in the bottom boundary layer. The total stress that was estimated from the combined XCP and XDP data is about 5 Pa at section C, with roughly equal contributions from entrainment stress and bottom stress. The combined stress represents a very significant brake on the outflow current, but it is only about one-third of the initial pressure force.

2) Entrainment has an additional, and in some respects decisive, effect on the outflow by reducing its density, and thus, the density anomaly. The outflow density is reduced to about $\sigma_\theta = 27.75$ kg m^{-3} by section D, and the density anomaly is reduced to about $\Delta\rho \approx 0.7$ kg m^{-3}, which is a little less than half of its value at section B. This halves the pressure force on the outflow.

3) Finally, the earth's rotation also limits the downhill acceleration of the outflow: the Coriolis force turns the current to the right (looking in the direction of the flow). Instead of flowing directly down the steepest slope, the outflow turns and flows more nearly parallel to isobaths (Fig. 1C). By following a column that was moving from section B to D, we estimated that the current turns at ~90° per 7 hours, which is comparable to the turning rate of an inertial current at this latitude (the Coriolis parameter f = 90° per 5.1 hours) (*26*).

The initial descent of the continental slope thus has the character of a geostrophic adjustment process in which the outflow current responds to an increased bottom slope (*27*). The increased pressure force accelerates the current enough to raise the Froude number above 1, and entrainment becomes intense. The consequent loss of density anomaly, together with the effect of geostrophic adjustment, limits this region of strong mixing to only a few tens of kilometers or, following the current, only a few hours. However, in this brief interval, the density of the outflow is reduced enough that, even if no further mixing occurred, the Mediterranean outflow would settle into the thermocline rather than the deep sea.

Damped geostrophic flow. As the outflow reaches sections E and F, it turns to flow nearly parallel to the bottom topography (Fig. 1C). The current speed is greatly reduced to about $U = 0.4$ m s^{-1}, and the current is then in a near geostrophic balance in which the Coriolis acceleration is roughly balanced by the across-stream topographic acceleration: $fU \approx g'd_y$, where $\Delta\rho \approx 0.5$ kg m^{-3} and $d_y \approx (8 \pm 3) \times 10^{-3}$ is the bottom slope normal to the current. If the Froude number of a geostrophic outflow is to exceed 1, then for the observed thickness and density anomaly, the bottom slope would have to satisfy $d_y \geq f\sqrt{h/g'} \approx 13 \times 10^{-3}$, which it does not near section F (*28*). The maximum observed Froude number is about 0.3, well below the level at which significant entrainment might be expected. The comparatively tranquil character of the flow is evident in the XCP and XDP profiles (Figs. 3 and 4), which show that the interfacial boundary layer has a much reduced thickness and turbulence intensity. This suggests that mixing between the outflow and Atlantic water is considerably reduced at sections E and F, which is consistent with the much slower rate of decrease of S_{Twtd} along the path in this region (Fig. 2C).

The turbulence in the bottom boundary layer is also much less intense in this region, and the bottom stress is about 0.3 Pa as estimated from XCP profile data along section F. This weaker but still significant bottom stress may play a crucial role in the longer term evolution of the outflow by providing the damping (dissipation) that allows the otherwise geostrophic current to descend the continental slope without accelerating. The effect of bottom friction on a nearly geostrophic current can be inferred from the ratio of the bottom stress to the across-stream (geostrophic) topographic acceleration, which is known as the Ekman number, $K = (\tau_b/\rho h)/(g'd_y)$, where $h \approx 100$ m and $\Delta\rho$ and d_y are as before. Thus, $K \approx 0.2$, which is the angle of the current, in radians, with respect to the isobaths. As the outflow moves from section F to Cape Saint Vincent, a distance L = 200 km, it can descend an additional depth $LKd_y \approx 200$ m without accelerating.

Our hydrographic data show that the outflow continues westward along the continental slope as a damped geostrophic current that slowly crosses isobaths. There is additional mixing, although the rate is much less than that found around section C, and when the outflow reaches Cape Saint Vincent and the open North Atlantic, it has properties that make it neutrally buoyant at depths of about 800 to 1300 m: $T = 12° \pm 1°C$, $S = 36.4 \pm 0.1$ psu, and $\sigma_\theta = 27.6 \pm 0.1$ kg m^{-3}.

Other North Atlantic Outflows

The lower, denser portion of the outflow floats off of the bottom in the western Gulf of Cadiz and forms the saline tongue that extends west across the North Atlantic basin (Fig. 1A) (29). The upper portion of the outflow continues north for some distance along the Iberian Peninsula and merges with a poleward eastern boundary undercurrent that carries the saline Mediterranean water toward the inflow of the Norwegian Sea, just west of Ireland. The relatively high salinity of the water that flows into the Norwegian Sea must enhance the density of the very cold waters that are produced there during the winter. Cold, dense water from the Norwegian Sea forms two important outflows (30–32) that form the deep and bottom water in the North Atlantic. By contributing to the salinity of the Norwegian Sea inflow (33), the warm, dry climate over the Mediterranean Sea may enhance the cold, thermally dominated circulation of the deep ocean (14).

The qualitative pattern of the mixing and dynamics found in the Mediterranean outflow—intense mixing during the initial descent of the continental slope followed by a long stretch of nearly geostrophic flow—may be discerned as well in historical observations of the Norwegian Sea outflow through the Denmark Strait (32). This outflow begins at the sill west of Iceland with properties that make it less dense than pure Mediterranean outflow water: $T = 0°C$, $S = 34.9$ psu, and $\sigma_\theta = 28.05$ kg m^{-3}. It flows southward along the continental slope of Greenland and entrains warmer, presumably overlying, water somewhere in the northern Irminger Sea, which is evident because it warms 1° to 2°C. This outflow loses only about 0.1 kg m^{-3} of its density by entrainment and remains just dense enough to become bottom water in the North Atlantic. The Denmark Strait outflow continues south for thousands of kilometers along the continental slope of North America as the deepest and densest portion of a geostrophic current called the Deep Western Boundary Current. This current mixes only very slowly with its surroundings (34) and retains its chemical identity at least as far south as the tropics.

Models of the general circulation that simulate a deep ocean that changes over time will probably need to include some representation of time-varying marginal sea outflows. There are at least two somewhat different problems posed by this: first, to specify or simulate the seawater properties of the marginal seas, and second, to allow the marginal seawater to flow out into the open ocean in a realistic manner. Our study gives some indications of what may be required for this second part. The geostrophic portion of an outflow current and the accompanying gradual changes in outflow properties would seem to present no special demands. However, the rapidly varying portion of an outflow path, for example, the first 100 km of the Mediterranean outflow where the transport doubles, will pose resolution and parameterization problems that appear to be unique to outflows. These particular portions of the outflows, which we think are localized around steep topography near the marginal sea, may have to be treated by a submodel (35) that has enhanced vertical resolution and mixing parameterizations which are appropriate to density currents.

REFERENCES AND NOTES

1. B. A. Warren, in *Evolution of Physical Oceanography, Scientific Surveys in Honor of Henry Stommel*, B. A. Warren and C. Wunsch, Eds. (MIT Press, Cambridge, MA, 1981).
2. J. A. Whitehead, *Sci. Am.* **260**, 50 (February 1989).
3. J. F. Price, *Oceanus* **35**, 28 (summer 1992).
4. Around 50 million years ago, the bottom water in the North Atlantic was much warmer than it is today (~15°C versus 2°C) and probably saltier as well [G. W. Brass, J. R. Southam, W. H. Peterson, *Nature* **296**, 620 (1982)]. This implies that the main source of deep water must have been tropical or subtropical rather than polar or subpolar, as it is today. Other evidence shows that the chemistry of the deep North Atlantic varied during periods of glaciation about 10,000 to 15,000 years ago, which implies at least a relative change in the properties of southern versus northern subpolar sources [H. Wang and G. E. Birchfield, *Clim. Dyn.* **8**, 49 (1992)].
5. The density of seawater is usually in the range $\rho = 1020$ to 1050 kg m^{-3} and is generally reported as $\sigma = \rho - 1000$, as is done here. When one compares the density of different water masses, it is appropriate to compare them at the same pressure; the notation σ_θ indicates that the reference pressure is at sea level. If density is instead computed at the in situ pressure of the deep sea, then pure Mediterranean water is roughly equal in density to North Atlantic bottom water because warm Mediterranean water is less compressible.
6. The salinity of the Mediterranean water is determined by the amplitude of this two-layer exchange and by the convection process, which mixes the water column vertically [H. L. Bryden and H. M. Stommel, *Oceanol. Acta* **7**, 289 (1984)]. It is characteristic of estuarine-like circulations that the transport in either layer, about 0.7×10^6 m^3 s^{-1} within the Strait of Gibraltar, is much larger than the freshwater loss, here about 0.05×10^6 m^3 s^{-1}, that initiates the exchange [H. L. Bryden, E. C. Brady, R. D. Pillsbury, in *Seminario Sobre la Oceanografia Fisica del Estrecho de Gibraltar*, J. L. Almazan, H. Bryden, T. Kinder, G. Parrilla, Eds. (Sociedad Espanola de Estudios para la Communicacion Fija a Traves del Estrecho de Gibraltar, Madrid, Spain, 1989), pp. 166–179]. The amplitude of the exchange with the North Atlantic is constricted by the shallow and narrow Strait of Gibraltar. A semi-enclosed sea like the Mediterranean will thus produce a smaller volume of more saline water than would a comparable open ocean region that is subject to the same freshwater loss.
7. By entrainment we mean vertical mixing that incorporates overlying North Atlantic water into the outflow layer. Because the North Atlantic water has a lesser salinity and density, entrainment also causes a decrease in the salinity and density of the outflow layer. Similarly, entrainment of eastward-flowing North Atlantic water causes an eastward stress. Entrainment also increases the volume transport of the outflow from about 0.7×10^6 m^3 s^{-1} within the Strait to about 2.5×10^6 m^3 s^{-1} in the western Gulf of Cadiz (9).
8. B. C. Heezen and G. L. Johnson, *Bull. Inst. Oceanogr. (Monaco)* **67**, 1 (1969).
9. J. Ochoa and N. A. Bray, *Deep-Sea Res.* **38**, 5465 (1991).
10. F. Madelain, *Cah. Oceanogr.* **22**, 43 (1970).
11. W. Zenk, *"Meteor" Forschungsergeb. Reihe A* **16**, 35 (1975).
12. I. Ambar and M. R. Howe, *Deep-Sea Res.* **26A**, 535 (1979).
13. M. R. Howe, *Oceanogr. Mar. Biol.* **20**, 37 (1982).
14. J. L. Reid, *Deep-Sea Res.* **26**, 1199 (1979).
15. M. A. Kennelly and J. H. Dunlap, *Technical Report No. APL-UW TR 8914* (Applied Physics Laboratory, University of Washington, Seattle, 1989).
16. An XCP measures the electric field created by seawater that is moving through the earth's magnetic field [T. B. Sanford, R. G. Drever, J. H. Dunlap, *Deep-Sea Res.* **25**, 183 (1978)] and can resolve vertical variations in ocean currents over scales of about 0.3 m and larger. The XCP data alone do not provide a measure of the depth-independent, or barotropic, current, which has to be determined in some other way. In this case, we estimated the barotropic current by requiring that there be no net salt transport through the sections. This requires that a small barotropic current be added to the XCP-measured current (less than 0.2 m s^{-1}) and yields a zero-crossing of the along-stream current that is 5 to 40 m below the top of the outflow, as determined by the deepest occurrence of pure North Atlantic water. This gives the result that some mixed water flows eastward, which we would expect in a stratified shear flow.
17. An XDP measures the fluctuation of hydrodynamic lift forces on a centimeter-scale piezo-ceramic transducer [T. R. Osborn and W. R. Crawford, in *Air-Sea Interaction: Instruments and Methods*, F. Dobson, L. Hase, R. Davis, Eds. (Plenum, New York, 1980), pp. 369–389] that is mounted on the nose of a probe that falls through the water column. Analysis of the data yields the one-dimensional spectrum of velocity shear over vertical scales from about 0.01 m, a high-frequency limit set by the transducer size, to about 0.5 m, a low-frequency limit set by the instrument size. This range includes most of the variance of turbulent shear. Turbulence that is highly dissipative may have some shear variance at even smaller scales, which we estimated by fitting the observed spectra to a universal spectrum [P. W. Nasmyth, thesis, University of British Columbia, Vancouver, Canada (1970)]. The estimated shear variance, $\langle U_z^2 \rangle$, is then used together with the isotropic dissipation formula to estimate the rate of kinetic energy dissipation, $\varepsilon = 7.5\rho_0\nu\langle U_z^2 \rangle$, where $\nu \approx 1.2 \times 10^{-6}$ m^{-2} s^{-1} is the kinematic viscosity of seawater.
18. Although the Mediterranean outflow shows very little interannual variability, it does have fast time scale variability of two kinds. There is a very large internal tidal variability in the central Strait of Gibraltar (19). We believe that the elevated level of Mediterranean water that we observed at the main sill (near 0 km downstream distance in Fig.

1A) is attributable to aliasing of tidal variability of that sort. There has also been observed a weekly time scale variation of the outflow current in the western Gulf of Cadiz, which may be attributable to the meandering of the current and eddy formation [M. L. Grundlingh, *"Meteor" Forschungsergeb. Reihe A* **21**, 15 (1981)]. To monitor this fast time scale variability, we obtained CTD profiles at several fixed sites west of section A that were revisited up to six times during the course of our week-long experiment. The resulting time series data showed little temporal variation of the outflow thickness or salinity in the eastern Gulf of Cadiz (less than 30% variation in thickness).
19. L. Armi and D. M. Farmer, *Prog. Oceanogr.* **21**, 1 (1988).
20. T. H. Ellison and J. S. Turner, *J. Fluid Mech.* **6**, 423 (1959).
21. J. E. Simpson, *Gravity Currents in the Environment and the Laboratory* (Halsted, New York, 1987).
22. W. Sturges, *J. Mar. Res.* **33**, 117 (1975).
23. L. J. Pratt, *J. Phys. Oceanogr.* **16**, 1970 (1986).
24. J. S. Turner, *Buoyancy Effects in Fluids* (Cambridge Univ. Press, Cambridge, 1973).
25. If the bottom boundary layer has a logarithmic profile, then the shear is $U_z = U_*/kz$, and the energy budget reduces to $\varepsilon = U_*^3/kz$, which can be evaluated from XDP data alone. The bottom stress estimated in this way is smaller by about a factor of 3 than the bottom stress estimated from the XCP data and profile method [similar to the result by R. K. Dewey and W. R. Crawford, *J. Phys. Oceanogr.* **18**, 1167 (1988)]. At this stage, we do not know whether this difference arises from physical, hydrodynamic effects that are not included in the simple model that is used in both techniques (thermal wind shear or form drag) or from the temporal intermittence of ε. Although the absolute values of bottom stress do not agree closely, there is nevertheless a high visual correlation between the two kinds of stress estimates.
26. There are ridges on the sea floor that run southeast to northwest and appear to steer the outflow through this turn. However, because the current turns at almost the rate of an inertial motion, we think that the ridges are depositional features that were produced by the current itself [also suggested in (*8*) for geological reasons], rather than geological features that just happen to lie beneath the outflow.
27. R. W. Griffiths, *Annu. Rev. Fluid Mech.* **18**, 59 (1986).
28. The bottom slope becomes much steeper in the western Gulf of Cadiz and may satisfy this inequality over some portions of the outflow that remain in contact with the bottom.
29. W. Zenk and L. Armi, *Deep-Sea Res.* **37**, 1805 (1990).
30. R. R. Dickson, E. M. Gmitrowicz, A. J. Watson, *Nature* **344**, 848 (1991).
31. P. M. Saunders, *J. Phys. Oceanogr.* **20**, 29 (1990).
32. J. H. Swift, *Deep-Sea Res.* **31**, 1339 (1984).
33. The entire subtropical North Atlantic has a significant net annual evaporation [R. W. Schmitt, P. S. Bogden, C. E. Dorman, *J. Phys. Oceanogr.* **19**, 1208 (1989)] that leads to a surface salinity maximum, although the salinities are considerably lower than those found in the Mediterranean Sea. This near-surface salinity maximum is advected toward the Norwegian Sea inflow by the North Atlantic current and appears to merge with the intermediate-level Mediterranean salinity maximum by a latitude of about 50°N. Thus, the high salinity of the inflow to the Norwegian Sea comes from both subtropical North Atlantic and Mediterranean sources, and, judging by the volume fluxes alone, the former may be the more important.
34. R. S. Pickart, *J. Phys. Oceanogr.* **22**, 1047 (1992).
35. P. C. Smith, *Deep-Sea Res.* **22**, 853 (1975).
36. C. Maillard, *Atlas Hydrologique de l'Atlantique Nord-est* [Institut Français de Recherche pour l'Exploitation de la Mer (IFREMER), Brest, France, 1986].
37. This research was supported by grants from the Office of Naval Research. We are grateful to J. H. Dunlap, T. W. Lehman, B. Brown, and J. Lynch for their help with the field experiment and the data analysis.